Proceedings of the 28th IEEE
EMBS Annual International Conference
New York City, USA, Aug 30-Sept 3, 2006

Microassembly Techniques for a Three-Dimensional Neural Stimulating Microelectrode Array

Y. Yao, *Member, IEEE*, M. N. Gulari, and K. D. Wise, *Fellow, IEEE*

Abstract—**This paper describes microassembly techniques for an out-of-plane three-dimensional microelectrode array for neural stimulating and recording in the central nervous system. An interlocking mechanism has been introduced into the microassembly components to facilitate the process, increase the robustness of the assembled device and improve the yield of the overall system. In-vivo testing has demonstrated full functionality of the microassembled 3D array.**

I. INTRODUCTION

Advances in MEMS technology have led to more and more complicated microsystems requiring the integration of different MEMS structures along with electronics and packaging [1, 2]. Some assembly procedures are frequently required to manipulate individual microparts to form complex but compact multi-dimensional systems [3]. The assembly processes at the microscale are usually very challenging and can be much less reliable and efficient than traditional automatic assembly in the macro domain. Various microassembly techniques [4, 5] and structures [6, 7] have been developed to achieve precise alignment and robust bonding between different components with automatic microassembly mechanisms.

In developing implantable neural microelectrodes, the requirements for microassembly are especially demanding due to the fact that the implanted devices should be minimally invasive to the target tissue. One approach to the assembly of separate electronic and MEMS components for a high-density microelectrode system has been investigated in [8]. Michigan Probes have taken a different approach, fabricating microelectrode structures and electronics on the same silicon wafer in an integrated monolithic process. A planar stimulating probe with on-chip CMOS circuitry was reported in [9]. This paper presents a set of out-of-plane microassembly techniques for constructing three-dimensional stimulating microelectrode arrays from fabricated planar structures. In the following sections, the microassembly procedures and different microassembly structures are described and analyzed. In-vivo testing of the assembled arrays is demonstrated in guinea pig models.

II. OVERVIEW OF MICROASSEMBLY PROCESS

The microassembly process for the 3D microelectrode array is illustrated in Fig. 1. The planar probe shown in (a) features integrated CMOS circuitry on the backend, separated from 8 penetrating shanks, each of which supports 8 IrO sites spaced 400µm apart for charge transfer between the probe and stimulated neural tissue. In between there are low-profile silicon/Au/parylene structures [10] with the ability to fold over at designated positions as shown in (b) to minimize the vertical rise and allow the dura to be replaced after implant. The Au beam leads on the outriggers of the probe are also bent to facilitate lead transfer [7] between the probe and platform. Multiple folded planar probes are mounted on a monolithically fabricated platform with matching holes in it for the probe shanks as in (c). After implantation, the platform supporting the upper portion of the probes sits on the cortical surface while the probe shanks penetrate the target neural tissue. Shown in (d), two vertical spacers are inserted into the flanges on the outriggers of each probe to fix the probes vertical with 400µm spacing. Two horizontal spacers are placed at the edges of the folded-down probe back-ends to hold them parallel to the platform surface. Finally a hybrid MOSIS chip is bonded to the platform for addressing the different probes. The system connects to a percutaneous plug through a flexible silicon ribbon cable or an integrated parylene cable.

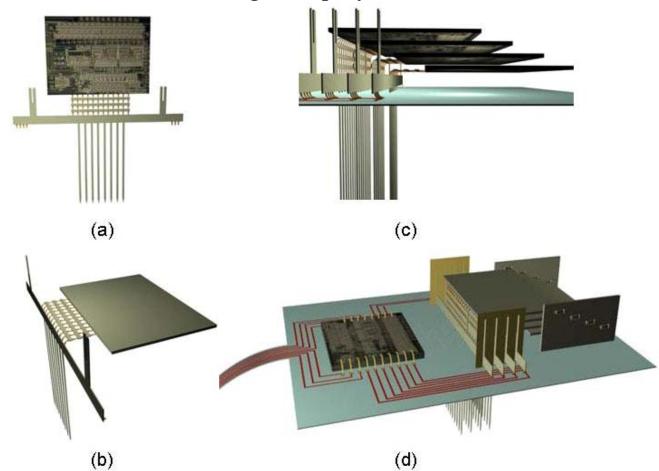

Fig. 1: Schematic of the microassembly of a 3D stimulating array.

II. DESIGN OF THE MICROASSEMBLY STRUCUTRES

To facilitate microassembly, an interlocking mechanism has been introduced into the process and three different micro-latching structures have been designed at the bottom of the spacers so that they can latch in the platform, fixing the mounted probes in place and holding the probes together with the platform. Their feasibility and design rules were analyzed, and ANSYS simulations were used to determine the dimensions of the final fabricated structures.

Manuscript received April 24, 2006. This work was supported by the NIH/NINDS Neural Prosthesis Program under contract NIH-NINDS-NO1-NS-9-2304.

The authors are with the Engineering Research Center for Wireless Integrated MicroSystems, University of Michigan, Ann Arbor, MI 48109-2122 USA.

1-4244-0033-3/06/$20.00 ©2006 IEEE.

A. Key Structure

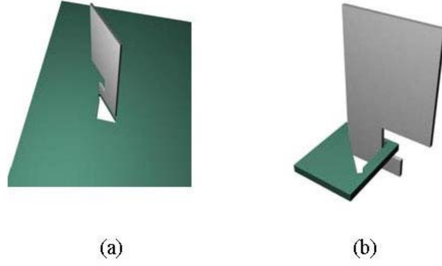

Fig. 2: Illustration of the key structure: (a) disengaged; (b) engaged.

The key structure shown in Fig. 2 operates like an ordinary latch key. The platform (green) has a triangular hole in it. The anchor (gray) can be inserted into the keyhole along the longest side and then rotated to 45º until it hits the short side of the hole and is latched into the platform. The key structure is easy to implement. The only drawback is that it requires enough space for key insertion and rotation without interfering with the other structures assembled on the platform. As a result, it is used only in the two horizontal spacers for holding the folded-down probe backends in position.

B. Snap Beam Structure

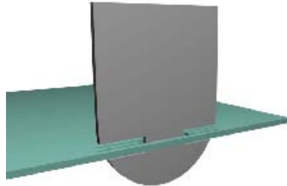

Fig. 3: Illustration of a snap-beam structure.

Illustrated in Fig. 3 is a snap-beam structure. It features two cantilever beams in the platform which can deflect and snap into slots in the anchor for engagement when the anchor is pushed down through the platform. The beam spring constant can be defined as

$$k = \frac{EWH^3}{4L^3},$$

where E is Young's modulus of the platform material and L/W/H are the length/width/thickness of the deflecting beams, respectively. Since the platform supports multiple microassembled structures, there is not much freedom in the dimensional parameters to optimize the elasticity of the cantilever beams. For L=50μm/W=12μm/H=12μm, ANSYS simulations show that with a displacement load of 39μm applied to the anchor, the maximum stress increases exponentially with the Young's Modulus. Shown in Fig. 4, with E=107GPa (corresponding to boron-doped silicon) the maximum stress is around 17.9GPa, much higher than the fracture stress for silicon (~500MPa). As a result, the snap beam design is not used in the 3D array.

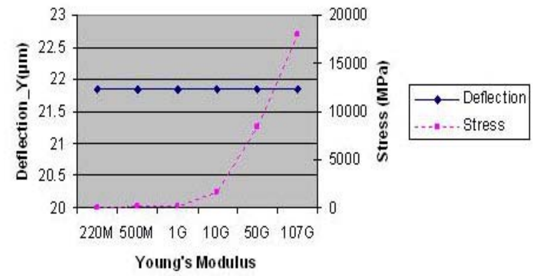

Fig. 4: Plot of stress and vertical deflection for different Young's moduli for the snap-beam structure.

C. Snap Fastener Structure

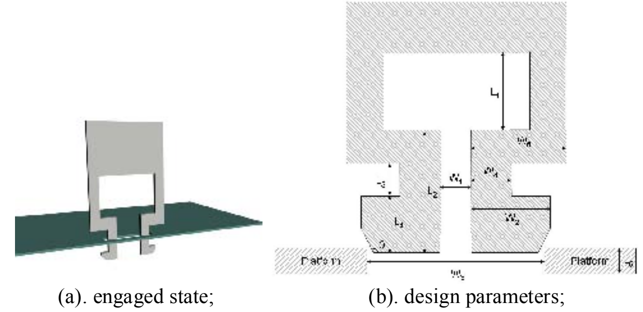

(a). engaged state; (b). design parameters;

Fig. 5: Illustration of a snap fastener structure.

The snap fastener shown in Fig. 5(a) features an anchor with a pair of barbed hooks that can deflect in the horizontal direction and snap into the hole in the platform when the anchor is pushed downward. Different from the snap beam, the deformable structures for the snap fastener are located in the anchor. The dimensions of the anchor structure are more important in the latching mechanism than those of the platform, which allows more freedom in optimizing microlatch engagement. Different parameters are labeled in Fig. 5(b). For engagement, they need to meet the following requirements:

1) $L_3 > L_5$: L_5 is approximately 12μm, defined by the boron diffusion depth in fabrication;
2) $W_3 < 2W_2 + W_1$: To prevent the anchor from sliding out of the platform;
3) $W_3 < 2W_5 + W_1$: In order to support the anchor sitting on top of the platform;
4) $W_3 \geq 2W_4 + W_1$: Under this condition the engaged components are relaxed without any deformation. For a tight engagement, a less strict rule with $W_3 > 2W_4 + W'$ applies, where W' is effective W_1 when the two barbs deflect and hit each other at the bottom;
5) $W_3 > 2W_2 + W'$: To enable the anchor to penetrate through the platform;

Table 1: Values of the design parameters of the snap fastener.

Parameters	Values(μm)	Parameters	Values(μm)
L_2	374	W_2	107
L_3	50	W_3	226
L_4	50	W_4	70
W_1	50	W_5	115

6) L_4: Since the engaged barbs protrude out of the platform along the cortical surface after implant, L_4 need to be small enough to avoid damage to the implant tissue;
7) L_1, L_2, W_5, θ: These parameters affect the deflection characteristic of the snap fastener. Their values are determined by mechanical simulation.

The design parameters are set accordingly as in Table 1 except for L_1, which is optimized with ANSYS simulation. Due to symmetry, only half of the structure is simulated. The Young's modulus is chosen as 107GPa and Poisson's ratio is 0.17 for deep-boron-doped silicon material. Fig. 6 shows the stress result with L_1 set to 110µm and a displacement load of 8µm applied on the top of the anchor. The maximum stress is about 675MPa, located at the root of the anchor. The curvature of the anchor also affects its deflection characteristics. Plotted in Fig. 7 are results with different L_1 values (110µm, 300µm, 539µm) for both sharp-edged and round-edged anchors. The stress decreases as L_1 increases. With L_1 large enough, curvature plays a negligible role in reducing the stress. With L_1 equal to 539µm, the maximum stress in both cases is close to 75MPa.

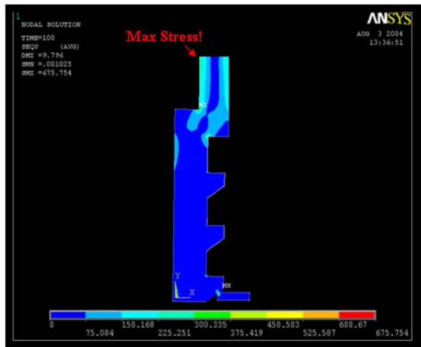

Fig. 6: ANSYS simulation of the stress for the snap fastener with L_1=110µm.

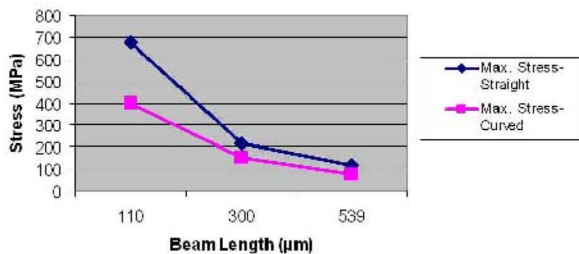

Fig. 7: Plot of the maximum stress and deflection vs. L_1 for sharp-edged and round-edged snap fastener.

III. Fabrication and Results

The integrated monolithic process to fabricate probes with CMOS circuitry is described in [10]. Fig. 8 shows a fabricated spacer equipped with a key structure and a snap fastener at each end and the bottom view of it engaged into the corresponding keyhole in the platform. The longer side of the key hole for key insertion measures 600µm, and the shorter side for key locking is 200µm to accommodate the corresponding dimensions for the key anchor of 490µm and 190µm, respectively. Two additional barbs are added to the snap fastener to compensate the variation in the heights of the mounted probes during assembly. This gives enough margin for all the assembled structures on the platform and helps build a tight and robust array. Experiments show that the spacer can easily snap into the platform and latches to hold the probes and facilitate subsequent assembly steps. A 3D microelectrode array has been constructed from 4 planar CMOS probes using these microassembly techniques and structures as shown in Fig. 9.

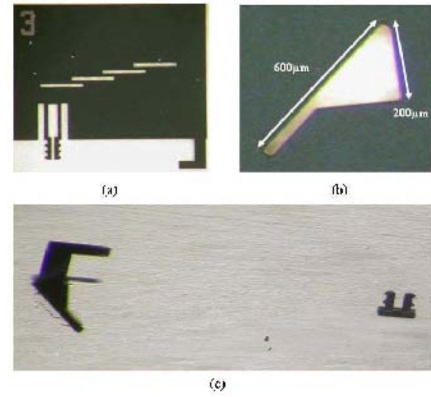

Fig. 8: Pictures of (a) a spacer with key structure; (b) the key hole in the platform and (c) the bottom view of an assembled spacer engaged in the platform.

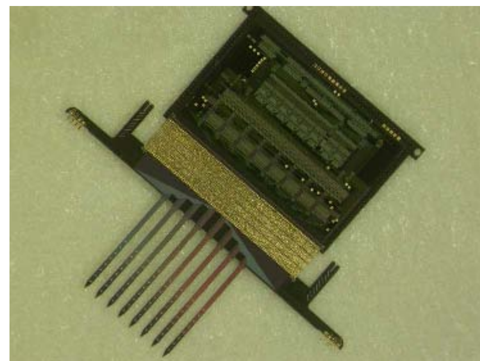

(a)

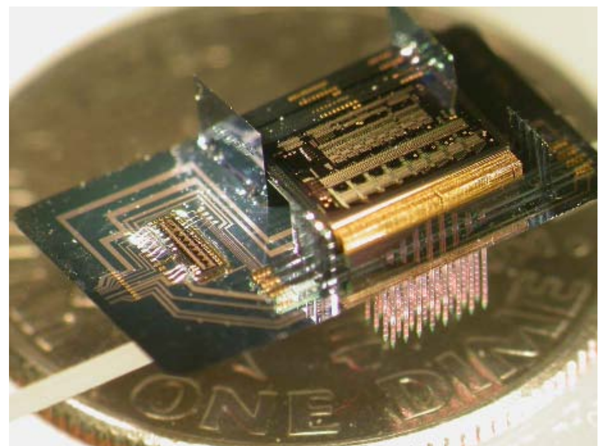

(b)

Fig. 9: Picture of (a) a planar CMOS probe and (b) a microassembled 4-probe microelectrode array.

IV. In-vivo Test Results

Before microassembly, the CMOS stimulating probe was tested in-vivo. It was implanted in the Dorsal Cochlear

Nucleus (DCN) of a guinea pig and programmed to generate symmetric biphasic current stimuli of 31µA every 250ms with 200µs pulse widths. A passive probe was placed in the Inferior Colliculus (IC) to record the neural responses projected from DCN. Shown in Fig. 10 are neural signals recorded from 6 different channels. Stimulated spike responses are detected behind a large stimulus artifact. After 100ms, only spontaneous neuron firing is observed.

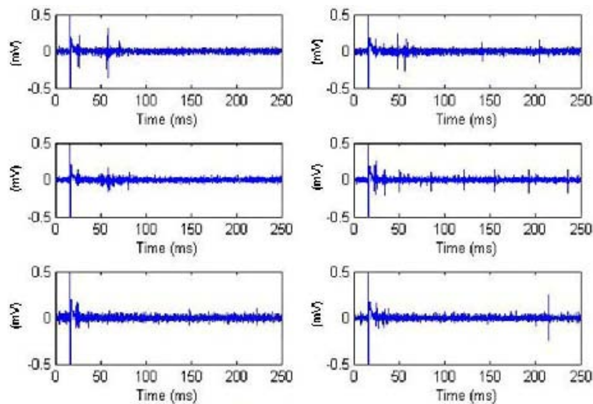

Fig. 10: Recorded neural responses from six different channels.

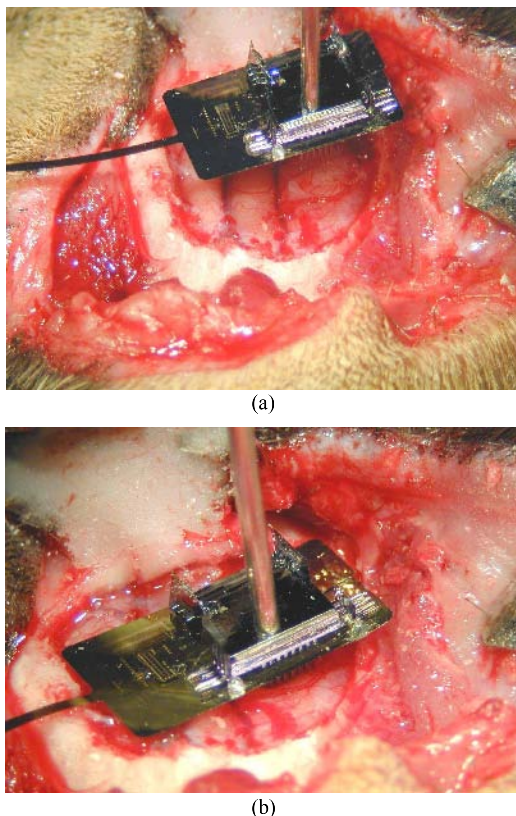

(a)

(b)

Fig. 11: Picture of a 3D microassembled stimulating array (a) before and (b) after being inserted in guinea pig auditory cortex.

Shown in Fig. 11(a) is a microassembled 4-probe array held with a vacuum pick just before being inserted into the auditory cortex of a guinea pig. By gently pushing the vacuum pick, the shanks penetrate through the pia into the tissue as shown in Fig. 11(b) even without the help of special insertion tools. The interlocking mechanisms not only simplify the assembly process of array, but also increase its robustness and improve the yield of the final system.

V. Conclusions

This paper has described and analyzed the microassembly techniques and structures needed to build a high-density three-dimensional microelectrode array from fabricated planar devices. The performance of the microassembled array has been demonstrated in-vivo. These techniques can be used for other MEMS applications requiring integration of separate devices to realize miniaturized fully-functional microsystems.

Acknowledgment

The authors wish to thank Ms. S. Ghimire for help with simulation and Mr. J. Wiler for assistance with in-vivo testing. This work made use of facilities supported by the Engineering Research Centers Program of the National Science Foundation under Award Number EEC-9986866.

References

[1] A. D. DeHennis and K. D. Wise, "A Wireless Microsystem for the Remote Sensing of Pressure, Temperature, and Relative Humidity," *J. Microelectromechanical Systems*, pp. 12-22, February 2005.

[2] B. H. Stark and K. Najafi, "A Low-Temperature Thin-Film Electroplated Metal Vacuum Package," *J. Microelectromechanical Systems*, pp. 147-157, April 2004.

[3] B. Nelson, Y. Zhou and B. Vikramaditya, "Sensor-Based Microassembly of Hybrid MEMS Devices," *IEEE, Control Systems Magazine*, pp. 35-45, December 1998.

[4] A. Singh, D. A. Horsley, M. B. Cohn, A. P. Pisano and R. T. Howe, "Batch Transfer of Microstructures Using Flip-Chip Solder Bonding," *J. Microelectromechanical Systems*, pp. 27-33, March 1999.

[5] N. Dechev, W. L. Cleghorn and J. K. Mills, "Microassembly of 3-D Microstructures Using a Compliant, Passive Microgripper," *J. Microelectromechanical Systems*, pp. 176-189, April 2004.

[6] R. Prasar, K. F. Böhringer and N. C. MacDonald, "Design, Fabrication, and Characterization of Single Crystal Silicon Latching Snap Fasteners for Micro Assembly," *Proc. ASME int. Mech. Eng.Congress and Exposition (IMECE'95),* San Francisco, CA, Nov, 1995.

[7] Q. Bai and K. D. Wise, "A High Yield Microassembly Structure for Three-Dimensional Microelectrode Arrays", *IEEE Trans. Biomed. Eng*., pp. 281-289, March 2000.

[8] Y. K. Song, W. R. Patterson, C. W. Bull, N. J. Hwang, A. P. Deangelis, C. Lay, J. L. McKay, A. V. Nurmikko, J. D. Donoghue, B. W. Connors, "Development of an Integrated Microelectrode /Microelectronic Device for Brain Implantable Neuroengineering Applications," *Proc. 26th Annual IEEE Int. EMBS Conf.*, pp. 4053-4056, San Francisco, September 2004.

[9] Y. Yao, M. N. Gulari, J. F. Hetke, and K. D. Wise, " A Low-Profile Three-Dimensional Neural Stimulating Array with On-chip Current Generation," *IEEE Int. Conf. in Medicine and Biology Society (EMBS '04)*, San Francisco, pp. 1994-1997, September 2004.

[10] Y. Yao, M. N. Gulari, S. Ghimire, J. F. Hetke, and K. D. Wise, "A Low-Profile Three-Dimensional Silicon/Parylene Stimulating Electrode Array for Neural Prosthesis Applications," *Proc. 27th IEEE Annual Int. EMBS Conf.,* pp. 1293-1296, Shanghai, September 2005.